# Integrated Metagenomics and Metabolomics Analysis Reveals Changes in the Microbiome and Metabolites in the Rhizosphere Soil of Different Varieties of *Thlaspi arvense* L.

Wenjie Zhang [+], Chao Fan [+], Lie Yang, Yan Sun [*], Lili Tang [*]

Posted Date: 9 February 2026

doi: 10.20944/preprints202602.0643.v1

Keywords: *Thlaspi arvense* L.; rhizosphere soil; metagenomics; metabolomics

 doi:10.20944/preprints202602.0643.v1



*Article*

# Integrated Metagenomics and Metabolomics Analysis Reveals Changes in the Microbiome and Metabolites in the Rhizosphere Soil of Different Varieties of *Thlaspi arvense* L.

**Wenjie Zhang [1,+], Chao Fan [2,+], Lie Yang [2], Yan Sun [1,*] and Lili Tang [2,*]**

[1] Heilongjiang Univ, Acad Modern Agr & Ecol Environm, Harbin 150080, Peoples R China

[2] Heilongjiang Academy of Agricultural Sciences, Harbin 150086, Peoples R China

* Correspondence: sunyan@hlju.edu.cn (Y.S.); tanglili19861126@126.com (L.T.)

[+] These authors contributed equally to this work and share first authorship.

**Abstract**

Pennycress (*Thlaspi arvense* L.), a representative and economically valuable cover crop, supports and enhances key ecological processes throughout its life cycle via its root system. It is hypothesized that pennycress selectively modulates its rhizosphere microbial community through root-derived metabolites, which may influence both the crop's growth and the subsequent crops in rotation. However, systematic investigations comparing the rhizosphere microbiomes and metabolomes among different pennycress lines remain limited. This study employed metagenomic and metabolomic approaches to examine the dynamic changes in the rhizosphere microbial community and metabolite profiles of three pennycress lines with significantly different total alkaloid contents. The goal was to elucidate the interactions between microbes and metabolites. Results indicated significant differences in microbial community structure across the cultivars. JiL67 maintained stable community diversity, while LiN54 (with the lowest alkaloid content) showed reduced diversity. HeL43 (with the highest alkaloid content) exhibited increased diversity but also potential community homogenization, accompanied by the significant enrichment of microbial taxa capable of alkaloid tolerance. Metabolomic analysis identified metabolites such as Portulacaxanthin II, Oleanolic acid, and Soraphen A as significantly enriched in the rhizosphere soil of pennycress. This study reveals the shifts in rhizosphere microbial communities and metabolites linked to different pennycress lines and uncovers their interactive mechanisms, providing a scientific foundation for developing more economically efficient pennycress cultivation strategies.

**Keywords:** *Thlaspi arvense* L.; rhizosphere soil; metagenomics; metabolomics

## 1. Introduction

Pennycress (*Thlaspi arvense* L.) is a diploid, annual, winter-hardy groundcover plant with abundant germplasm resources. It demonstrates remarkable ecological adaptability and cold tolerance, thriving in various regions and habitats worldwide. As an economic groundcover crop, it holds significant potential for widespread application [1]. Its active root system supports essential ecological processes year-round, offering a practical and effective solution for advancing sustainable agriculture [2–5]. Pennycress grows well in diverse climates but is most commonly found in temperate regions. Its cold tolerance makes it an ideal candidate for use as a fall-planted cover crop in the U.S. Midwest's maize-soybean rotation system. Pennycress provides several agronomic and economic benefits: 1) As a cover crop, it improves soil structure while reducing erosion and nutrient loss [6]. 2) Pennycress field residues do not significantly impact the fatty acid content or overall biomass of subsequent soybean crops [7] and effectively suppress weed seed germination and growth

 doi:10.20944/preprints202602.0643.v1



[8]. 3) The crop offers an additional revenue stream for farmers. Its seeds, rich in oil (27–39%), are used in soap and lubricant production and serve as a high-quality feedstock for biodiesel production [9]. Additionally, both the whole plant and tender shoots are utilized for food and medicinal purposes. Due to its content of secondary metabolites such as glucosinolates, alkaloids, and coumarins, pennycress is recognized in traditional Chinese medicine for its liver-clearing, vision-improving, digestive-regulating, diuretic, detoxifying, and anti-swelling properties [10]. Despite its substantial economic value, pennycress has long been regarded as a weed in China, hindering its resource development and utilization [11]. Consequently, it is crucial to conduct systematic research on the interactions between pennycress and soil microorganisms, as well as the biosynthesis regulation of its specific metabolites. Such research will provide the theoretical foundation and technical roadmap for its resource utilization.

Plant secondary metabolites are central to chemical defense mechanisms. Among these, allelopathic compounds such as alkaloids, terpenoids, and phenolics play key roles in plant adaptation and defense, enhancing resistance to both biotic and abiotic stresses [12,13]. In plant defense responses, the activation of the jasmonic acid (JA) signaling pathway triggers the coordinated expression of downstream defense genes, driving the synchronous accumulation of secondary metabolites such as terpenoids and alkaloids [14]. The rhizosphere is a key micro-environment where plant-soil interactions occur, serving as a primary site for plant secondary metabolism and energy transformation [15]. Root exudates, such as alkaloids, amino acids, and terpenoids, play a significant role in plant-microbe interactions by attracting and promoting the enrichment of specific microorganisms through mechanisms like structuring, recruitment, and interference. These interactions, in turn, modify the plant's metabolic profile, enhancing crop yields and the content of bioactive compounds while suppressing pathogenic or harmful microbes [16–18]. Rhizosphere microorganisms, as integral components of the microbiome, are pivotal for plant growth and development, biocontrol of pests and diseases, and the accumulation of secondary metabolites [3,19,20]. For example, the core microbial community of the citrus rhizosphere regulates microbe-plant and microbe-microbe interactions, facilitates nutrient acquisition, and promotes plant growth [21]. In sorghum's early growth stages, stochastic processes significantly influence fungal communities [22]. Rhizosphere microorganisms can also directly inhibit pathogen growth by synthesizing and secreting antimicrobial substances, such as polyketides and terpenoids, serving as an effective disease control mechanism [23,24]. Furthermore, microbial communities can shape host plant metabolism [25]. Thus, understanding the dynamics of the crop rhizosphere microbiome and metabolome is essential for optimizing production practices [26].

This study selected three pennycress accessions with significantly different total alkaloid contents from domestic and international germplasm collections for a three-year continuous cultivation trial. By systematically evaluating key agronomic traits and analyzing the rhizosphere soil microbiome and metabolome, the study aims to elucidate how different pennycress lines influence the rhizosphere microenvironment. The results will provide a theoretical foundation for breeding new pennycress varieties, developing tailored cultivation practices, and advancing the industrial application of bioherbicides or microbial inoculants derived from specific metabolites.

## 2. Materials and Methods

### *2.1. Experimental Materials*

The three pennycress germplasm accessions selected for this study, designated JiL67, LiN54, and HeL43, were sourced from Jilin, Liaoning, and Heilongjiang provinces in China. A three-year field trial was conducted at the Minzhu Experimental Station of the Heilongjiang Academy of Agricultural Sciences in Harbin (45°49′N, 126°48′E). Each accession was replicated three times, with an unplanted control plot, resulting in a total of 12 plots (20 m × 20 m = 400 m$^2$), spaced 2 meters apart. Seeds were sown on 1 September over three consecutive years, with a seeding rate of 1.5 kg/ha and a planting depth of 0.5 cm. All plots were uniformly managed, and plants were harvested around 20 June in the

 doi:10.20944/preprints202602.0643.v1



second year after overwintering. Aboveground biomass and rhizosphere soil samples were collected on 10 June 2025 (the third year).

*2.2. Measurement Indicators and Methods*

At pennycress maturity, a 1 $m^2$ quadrat was harvested from each plot. The fresh biomass was immediately weighed, and the number of plants within the quadrat was recorded to calculate the fresh weight per plant. Plant height was measured from the cotyledon scar to the apex of the primary branch. After air-drying to a constant weight, dry weight per plant was calculated. Three representative plants from each pennycress line were selected for biochemical analysis. Protein content was quantified using the BCA Protein Assay Kit (ADS-W-SP002), and total alkaloid content was determined using the corresponding kit (ADS-W-QT016), following manufacturers' instructions.

Three replicates were set up for each line. Rhizosphere soil was sampled using the five-point method: the root zone at a 0–10 cm depth was excavated with a trowel. Roots were carefully removed, and the adhering rhizosphere soil was collected by gently shaking the roots (the root-shaking method). The soil samples were sieved through a 20-mesh sieve, placed in centrifuge tubes, flash-frozen in liquid nitrogen, and stored at −80 °C for subsequent microbial community and metabolite analyses.

*2.3. Metagenome Sequencing and Analysis*

DNA was extracted from the soil samples using the E.Z.N.A.® Viral DNA Kit, following the manufacturer's protocol. The concentration and purity of the extracted DNA were measured using a NanoDrop 2000 instrument, and its quality was assessed by 1% agarose gel electrophoresis. DNA samples meeting quality criteria (OD260/280 = 1.8–2.2, OD260/230 ≥ 2.0) were stored at –80 °C for library construction. Sequencing libraries were prepared using the NEB Next® Ultra™ DNA Library Prep Kit for Illumina and sequenced by BMK Cloud Technology (Wuhan) Co., Ltd. Qualified DNA was fragmented into ~350 bp segments using a Covaris S2 ultrasonicator. The fragmented DNA underwent end repair, A-tailing, adapter ligation, size selection, PCR amplification, and purification to generate the final library. After QC, the libraries were sequenced on an Illumina NovaSeq 6000 platform to generate 150 bp paired-end reads.

*2.4. Untargeted Metabolomics Assays in the Rhizosphere Soil of the Field Pennycress*

For metabolite extraction, 50 mg of soil was weighed into a 2 mL tube. One milliliter of extraction solution (methanol/acetonitrile/water, 2:2:1, v/v/v) containing an internal standard (20 mg/L) was added, and the mixture was vortexed for 30 s. Steel beads were then added, and the sample was homogenized at 45 Hz for 10 min, followed by ultrasonic treatment for 10 min in an ice-water bath. The sample was incubated at –20 °C for 1 hour and then centrifuged at 12,000 rpm (4 °C) for 15 min. A 500 µL aliquot of the supernatant was transferred to a microcentrifuge tube and dried in a vacuum concentrator. The dried metabolites were reconstituted in 160 µL of solvent (acetonitrile/water, 1:1, v/v), vortexed for 30 s, ultrasonicated on ice for 10 min, and centrifuged again (12,000 rpm, 4 °C, 15 min). Finally, 120 µL of the supernatant was transferred to an injection vial. For QC, 10 µL from each sample was pooled to create a QC sample. Metabolomic analysis was performed using an LC-MS/MS system consisting of a Waters Acquity I-Class PLUS UPLC coupled to a Waters Xevo G2-XS QToF mass spectrometer. Separation was achieved using a Waters Acquity UPLC HSS T3 column (1.8 µm, 2.1 × 100 mm).

*2.5. Data Analysis*

After data preprocessing in Microsoft Excel 2019 (Version 2207; Microsoft Corp.), statistical analyses were conducted using IBM SPSS Statistics (Version 23), including one-way ANOVA and Duncan's multiple comparison tests ($P < 0.05$). Data were further analyzed and visualized with GraphPad Prism 2023 to illustrate changes in key indicators. Figures for metagenomic results were

 doi:10.20944/preprints202602.0643.v1



generated using ChiPlot and the BMKCloud platform. For both microbial community and metabolomic data, multiple comparison corrections were applied to control the false discovery rate (FDR).

Metabolomic profiling was performed using LC-MS/MS. Raw data, acquired with MassLynx V4.2, were processed using Progenesis QI software for peak picking, alignment, and annotation against the online METLIN database and a custom-built library. After normalizing peak areas to the total ion count, subsequent analyses were conducted. Principal component analysis (PCA) and Spearman correlation analysis were used to evaluate intra-group repeatability and quality control (QC) sample stability. Compound identities were cross-referenced against the Kyoto Encyclopedia of Genes and Genomes (KEGG) (http://www.genome.jp), Human Metabolome Database (HMDB) (https://hmdb.ca/), and LIPID MAPS Structure Database (Lipidmaps) (https://lipidmaps.org/) for classification and pathway information. Based on group assignments, fold changes (FC) were calculated and compared, and Student's t-test was applied to determine significance (p-value) for each compound. Orthogonal partial least squares-discriminant analysis (OPLS-DA) was performed using the ropls R package, with model validity confirmed by 200 permutation tests. Variable importance in projection (VIP) scores were derived from multiple cross-validation. Differential metabolites were identified using thresholds of FC > 1, p-value < 0.05, and VIP > 1. Enrichment of these metabolites in KEGG pathways was assessed using a hypergeometric test.

## 3. Results

### *3.1. Agronomic Traits and Physiological Indicators*

The agronomic traits and physiological indicators of the three pennycress lines are summarized in Table 1. HeL43 exhibited the highest mean values for the dry-to-fresh weight ratio (D/F) and protein content. However, no significant differences were observed among the lines in terms of plant height, D/F, or protein content. In contrast, HeL43's total alkaloid content (2646.05 μg/g) was significantly higher ($P < 0.05$) than that of JiL67 (1497.30 μg/g) and LiN54 (1400.95 μg/g).

**Table 1.** Agronomic traits and physiological indicators.

| Varieties | Plant Height (cm) | Fresh weight (g) | Dry weight (g) | D/F Ratio (%) | Protein content (mg/g) | Total alkaloids (mg/g) |
|---|---|---|---|---|---|---|
| JiL67 | 64.00 ± 9.64a | 53 | 15.25 | 0.30 ± 0.05a | 150.68 ± 19.73a | 1.50 ± 0.40b |
| LiN54 | 74.67 ± 20.01a | 40.35 | 13.55 | 0.35 ± 0.05a | 161.15 ± 5.10a | 1.40 ± 0.49b |
| HeL43 | 67.33 ± 3.06a | 41.1 | 15.17 | 0.37 ± 0.05a | 173.42 ± 1.44a | 2.65 ± 0.06a |

Different letters following numerical values indicate significant differences ($P < 0.05$), while identical letters denote no significant differences ($P > 0.05$).

### *3.2. Variation in the Rhizosphere Microbial Community Across Pennycress Lines*

After QC, Illumina high-throughput sequencing generated a total of 79,472,134,434 clean reads. For all samples, Q30 scores exceeded 92% (Supplementary Table 1), confirming the high accuracy of the sequencing data. Rarefaction curves for each sample plateaued, indicating that the sequencing depth was sufficient to capture the microbial diversity present (Supplementary Figure 1). Alpha diversity analysis of the soil microbial community is presented in Figure 1. For JiL67, neither the Shannon nor the Chao 1 index showed significant changes ($p > 0.05$), indicating stable overall community diversity. In contrast, cultivation of LiN54 resulted in significant reductions in both the Shannon index ($p < 0.05$) and Pielou's evenness index ($p < 0.01$), reflecting a decrease in diversity, while the Chao 1 index remained unchanged, suggesting no shift in species richness. After HeL43 cultivation, both the Shannon index ($p < 0.05$) and Pielou's evenness index ($p < 0.01$) increased significantly, while the Chao 1 index declined ($p < 0.05$). This suggests that the observed increase in community diversity was largely driven by enhanced evenness rather than richness. These changes

 doi:10.20944/preprints202602.0643.v1



indicate a homogenization process within the community, characterized by a more uniform species distribution, likely due to selection against rare species.

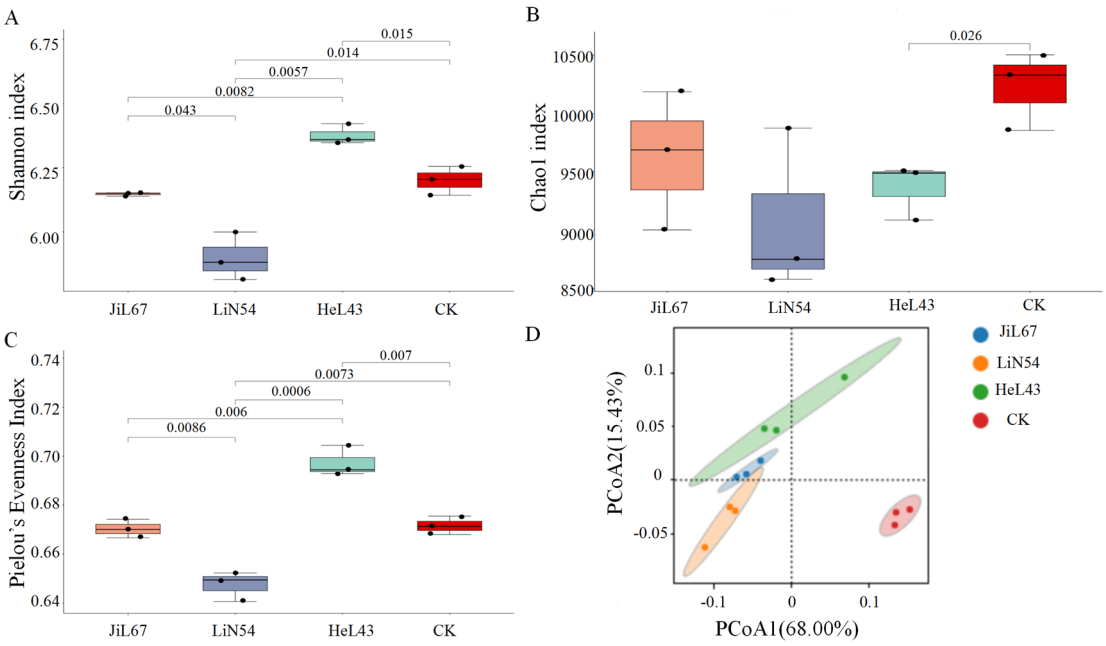


**Figure 1.** Microbial community diversity in pennycress samples. (A) Shannon index. (B) Chao1 index. (C) Pielou's Evenness Index. (D) Microbial community clustering diagram based on Bray-Curtis PCoA.

Principal coordinate analysis (PCoA) revealed clear separation among the four groups, with PCoA1 and PCoA2 explaining 68.00% and 15.43% of the variance, respectively (Figure 1D). This indicates that inter-group differences were the primary driver of microbial community variation, with HeL43 exhibiting the greatest separation. This pattern was strongly supported by ANOSIM based on Bray-Curtis distances ($R = 0.809$, $p = 0.001$; Supplementary Figure 2), confirming significant structural differences between groups. These results demonstrate that pennycress cultivation significantly altered the composition of the soil microbial community.

### *3.3. Composition of the Rhizosphere Microbial Community Across Pennycress Lines*

At the phylum level of microbial communities, bacteria dominate the rhizosphere soil (Figure 2A). In the control soil (CK), Actinobacteria, Proteobacteria, and Chloroflexi were the dominant phyla. In contrast, the dominant phyla in the pennycress-planted soils (JiL67, LiN54, and HeL43) were Proteobacteria, Actinobacteria, and Acidobacteria (Figure 2B). To facilitate an in-depth analysis of bacterial community variation across the pennycress lines, the communities were profiled at the genus level. A total of 2,516, 2,524, 2,464, and 2,551 genera were detected in the JiL67, LiN54, HeL43, and CK groups, respectively (Figure 2D). Across the four groups, the top ten genera in terms of abundance were largely consistent, though their relative abundances varied (Figure 2C). In CK, *Solirubrobacter*, *Nocardioides*, *Gaiella*, *Bradyrhizobium*, and *Blastococcus* exhibited relatively higher abundances. In JiL67, *Nocardioides*, *Nitrospira*, *Variovorax*, *Solirubrobacter*, and *Bradyrhizobium* exhibited higher relative abundances. In the LiN54 group, *Nocardioides*, *Nitrospira*, *Haliangium*, *Solirubrobacter*, and *Variovorax* exhibited relatively high abundances. In HeL43, *Nocardioides*, *Solirubrobacter*, *Nitrospira*, *Arthrobacter*, and *Variovorax* were the most abundant genera. LEfSe analysis revealed significant differences in the relative abundance of microbial communities between each of the three pennycress-planted groups and CK (Figure 2E, 2F). LEfSe identified a total of 34 biomarkers (LDA score > 4.0) across the four sample groups. Specifically, the CK community comprised 14 taxonomic units, with Actinobacteria being the primary contributor. The JiL67 community contained 3 units, predominantly from the family Comamonadaceae. The LiN54 community included 14 units, with

 doi:10.20944/preprints202602.0643.v1



major contributions from the class Betaproteobacteria, genus *Nitrospira*, order Myxococcales, class Deltaproteobacteria, and family Nitrospiraceae. The HeL43 community comprised 3 units, primarily contributed by the order Micrococcales. In the primary enriched communities of the rhizosphere, a positive correlation was observed between Nitrospirae and beneficial bacteria such as Acidobacteria and Candidatus Rokubacteria, while Actinobacteria showed a negative correlation with Nitrospirae.

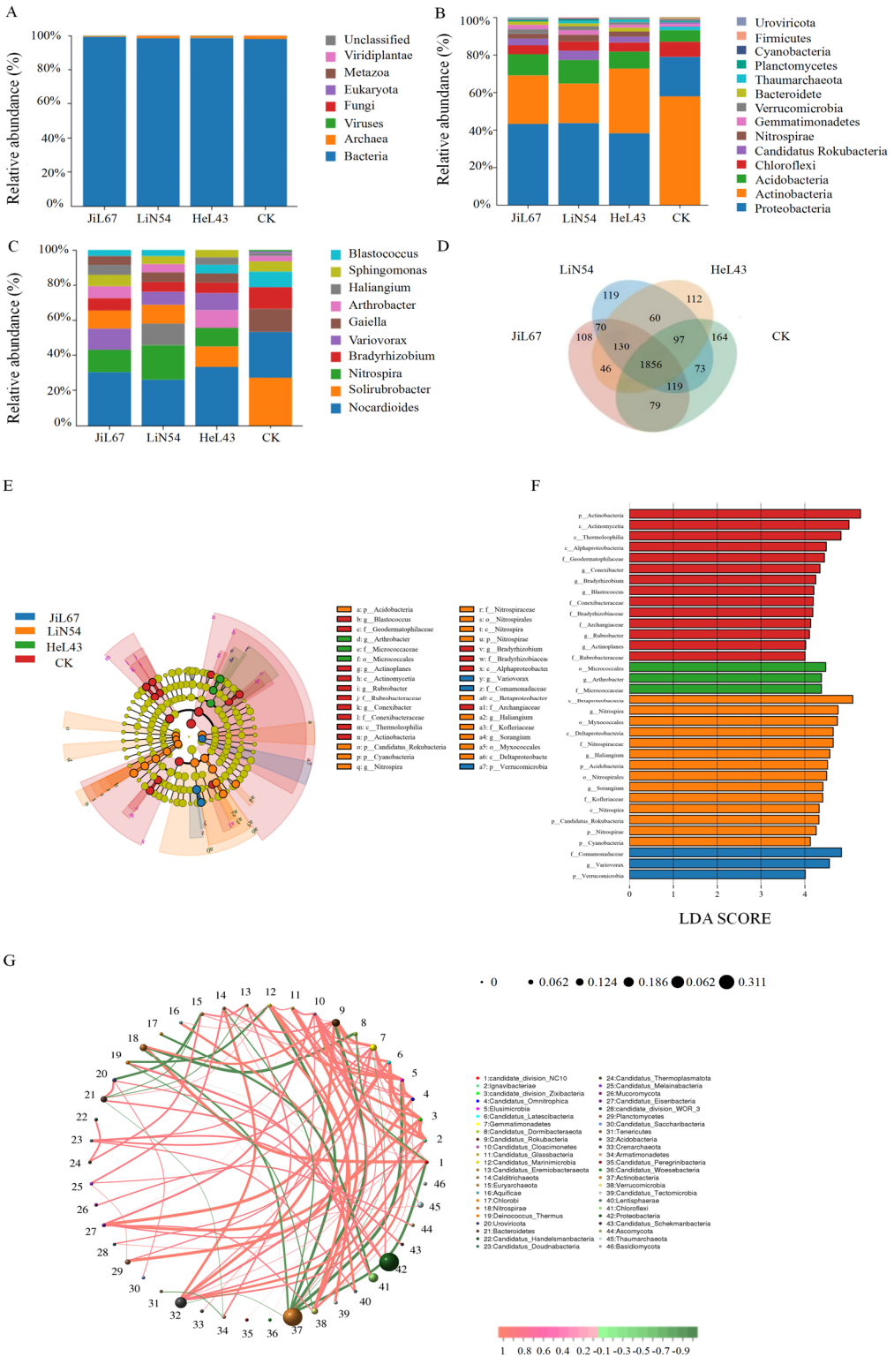

 doi:10.20944/preprints202602.0643.v1



**Figure 2.** Composition of microbial community in field pennycress samples. (A) Phylum-level composition of the rhizosphere soil microbial community. (B) Genus-level composition of the rhizosphere soil microbial community (Top 10 genera shown). (C) Venn diagram depicting the overlap of genera across different groups. (D and E) Cladograms from LEfSe analysis showing microbial taxa with differential abundance across groups at various taxonomic levels. (F) Correlation network analysis of microbial taxa in different groups.

### *3.4. Potential Functional Pathways of the Rhizosphere Microbiome Across Pennycress Lines*

As shown in Figure 3A, the four soil sample groups were assigned to a total of 169 KEGG level 3 pathways, with 160, 166, 161, and 167 pathways detected in JiL67, LiN54, HeL43, and CK, respectively. Notably, LiN54 harbored two unique pathways: Glycosphingolipid biosynthesis - ganglio series and Glycosphingolipid biosynthesis - globo and isoglobo series. Conversely, CK contained two distinct pathways: Mitophagy – yeast and SNARE interactions in vesicular transport. Based on annotation results (Figure 3B), significant differences in potential functions were observed across the four groups, particularly in: Glycolysis/Gluconeogenesis, Homologous recombination, Arginine biosynthesis, Porphyrin and chlorophyll metabolism, and Terpenoid backbone biosynthesis. Additionally, the relative abundances of genes involved in ketone body synthesis and degradation, aminobenzoate degradation, fluorobenzoate degradation, and polycyclic aromatic hydrocarbon degradation were significantly higher after pennycress cultivation. A heatmap of the top 30 differentially abundant functional pathways is shown in Figure 3C. The results revealed that after pennycress cultivation, the JiL67 group was enriched in Propanoate metabolism, Valine, leucine, and isoleucine degradation, and Fatty acid metabolism. The LiN54 group exhibited enrichment in 2-Oxocarboxylic acid metabolism, RNA degradation, and Pyrimidine metabolism. In the HeL43 group, enrichment was observed in Microbial metabolism in diverse environments, Pyruvate metabolism, and Glyoxylate and dicarboxylate metabolism.

 doi:10.20944/preprints202602.0643.v1



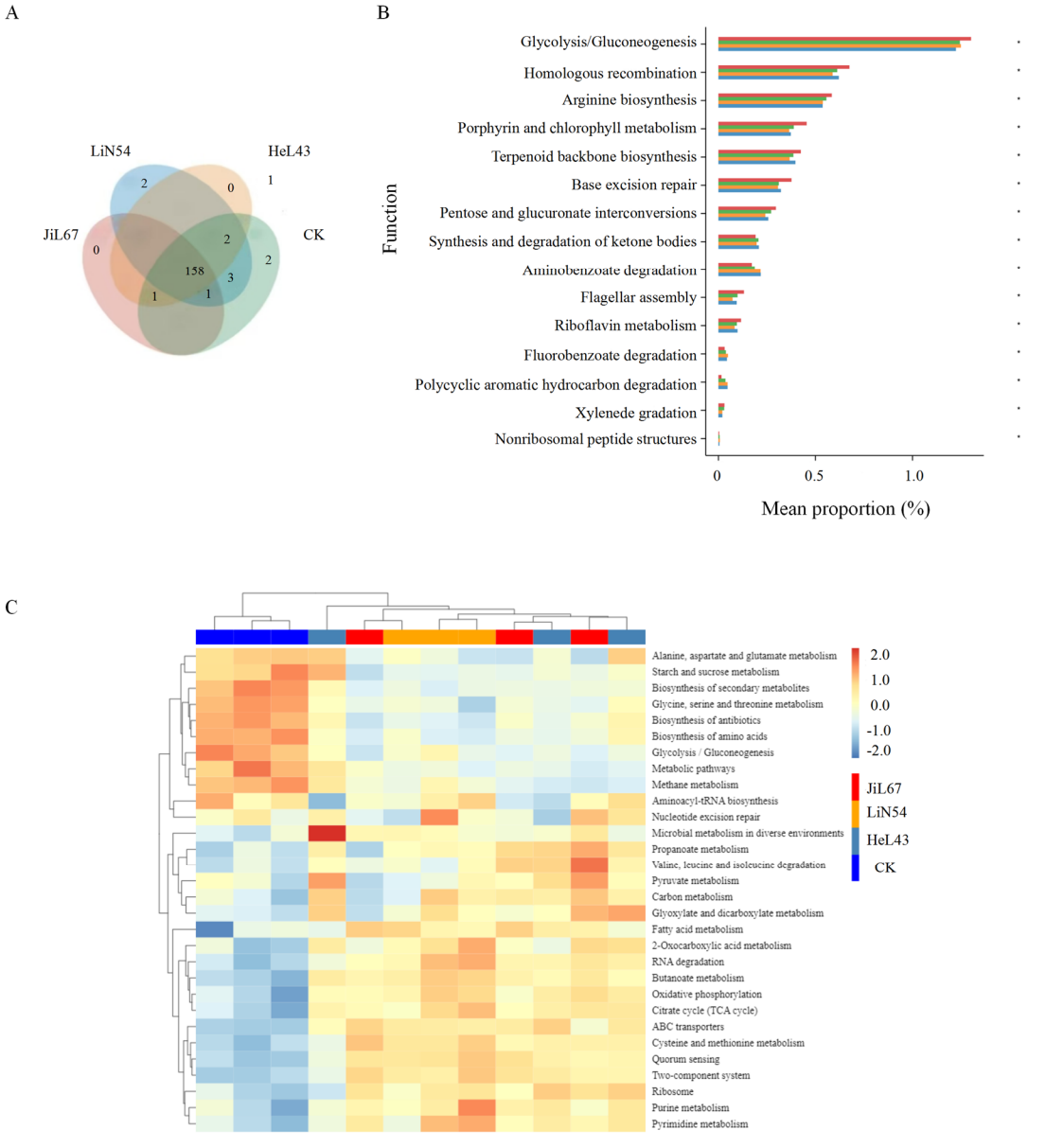


**Figure 3.** Analysis of potential functional pathways in soil microorganisms. (A) Venn diagram of KEGG level 3 pathways across all samples. (B) Bar chart showing the top 15 significantly different functions based on the Wilcoxon rank-sum test. For each function, the left bar indicates mean relative abundance (x-axis), the center shows significance level (*, $P < 0.05$; **, $P \leqslant 0.001$; ***, $P \leqslant 0.0001$), and the right number represents the exact P-value. Functions are ranked first by P-value (descending) and then by abundance (highest to lowest).(C) Heatmap of the top 30 differentially abundant functional pathways.

### *3.5. Non-Targeted Soil Metabolite Analysis*

Correlation analysis between the three pennycress lines and the control soil samples revealed correlation coefficients greater than 0.88, indicating a high similarity in metabolite expression levels across the samples (Supplementary Figure 3). According to the HMDB database (covering the top 20 categories by metabolite count), the primary metabolites in pennycress rhizosphere soil included fatty acyls, organooxygen compounds, carboxylic acids and derivatives, prenol lipids, steroids, and steroid derivatives (Figure 4A).

 doi:10.20944/preprints202602.0643.v1



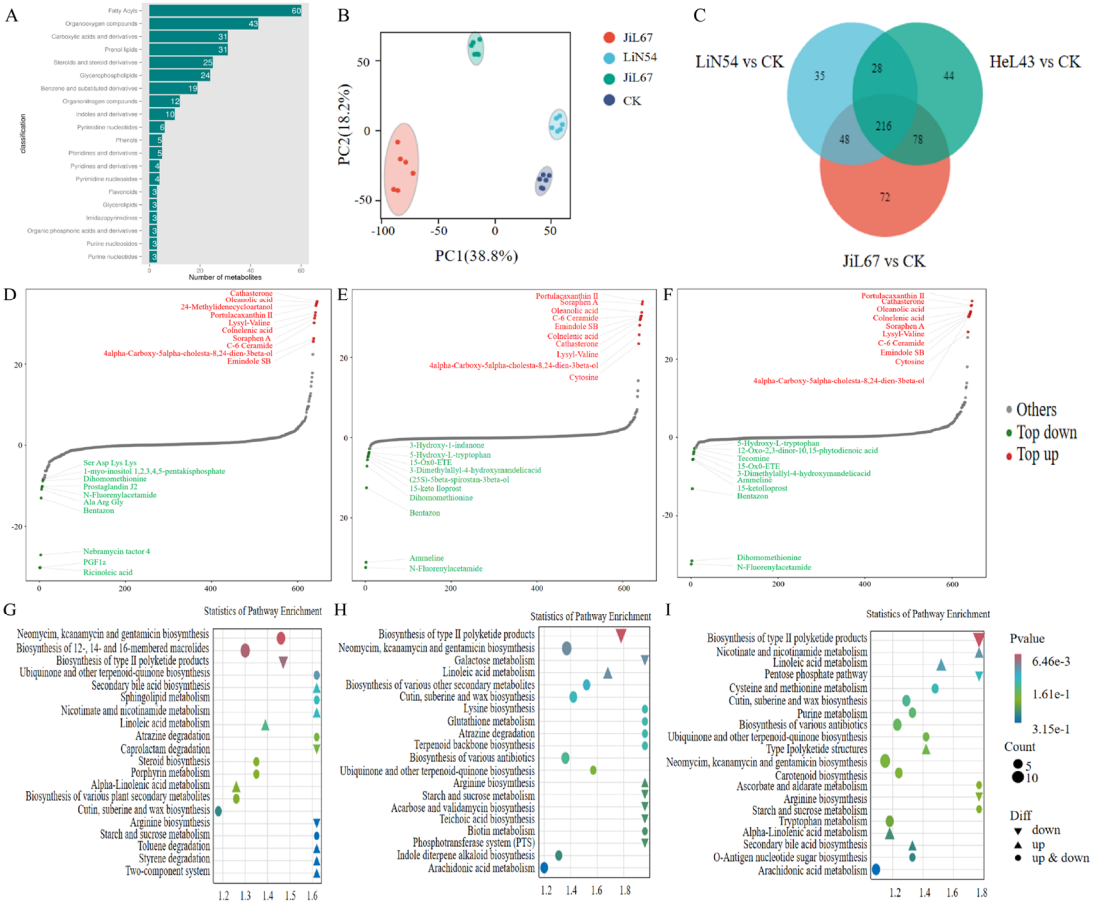


**Figure 4.** (A) Primary metabolites in the rhizosphere soil of Cynoglossum officinale. (B) PCA of metabolites across four groups. (C) Venn diagram of differentially expressed metabolites. (D) Dynamic distribution map of metabolite content differences between CK and JiL67. (E) Dynamic distribution map of metabolite content differences between CK and LiN54. (F) Dynamic distribution map of metabolite content differences between CK and HeL43. The horizontal axis represents the cumulative number of substances sorted by fold change in ascending order, while the vertical axis displays the logarithm of fold change to base 2. Each point represents a substance: green points indicate the top 10 downregulated substances, and red points represent the top 10 upregulated substances. (G) Metabolic pathway enrichment analysis diagram for CK versus JiL67. (H) Metabolic pathway enrichment analysis for CK versus LiN54. (I) Metabolic pathway enrichment analysis for CK versus HeL43. Each point in the diagram represents a KEGG pathway, with the x-axis denoting the enrichment factor (Rich_factor) and the y-axis showing the pathway name. The depth of dot color indicates P-value significance, while circle size represents the number of differentially enriched metabolites within the pathway. Dot shape indicates the direction of differential metabolism within the pathway: an upward-pointing triangle indicates all metabolites are upregulated, a downward-pointing triangle indicates all are downregulated, and a circle signifies the presence of both up- and downregulated metabolites. Pathways positioned near the top-right corner of the diagram provide greater reference value.

PCA showed significant differences in rhizosphere soil metabolite composition among JiL67, LiN54, HeL43, and CK groups (Figure 4A). The first two principal components, PC1 and PC2, explained 38.8% and 18.2% of the total variance, respectively. Differential metabolite analysis between the control soil and the three pennycress lines revealed distinct metabolic profiles. A total of 414, 327, and 366 differentially expressed metabolites (DEMs) were identified in comparisons with JiL67, LiN54, and HeL43, respectively (Supplementary Figures 4–6). Notably, the number of upregulated DEMs was significantly greater than the number of downregulated DEMs in all three lines (Supplementary Table 2). Venn diagram analysis (Figure 4C) indicated that 216 differential

 doi:10.20944/preprints202602.0643.v1



metabolites were common to all three pennycress lines when compared to the CK control. This suggests that the differences among pennycress samples were primarily due to metabolite abundance rather than compositional profile.

FC values for metabolites were calculated for each comparison group, and metabolites were then sorted in ascending order of FC to generate a dynamic distribution plot of metabolite differences. Compared to CK, metabolites such as Cathasterone, Oleanolic acid, 24-Methylidenecycloartanol, Portulacaxanthin II, and Lysyl-Valine were significantly upregulated in JiL67, while others, including Ricinoleic acid, PGF 1a, Nebramycin factor 4, Bentazon, and Ala Arg Gly, were significantly downregulated (Figure 4D). In LiN54, metabolites such as Portulacaxanthin II, Soraphen A, Oleanolic acid, C-6 Ceramide, and Emindole SB were significantly upregulated, while N-Fluorenylacetamide, Ammeline, Bentazon, Dihomomethionine, and 15-keto lloprost were significantly downregulated (Figure 4E). In HeL43, metabolites such as Portulacaxanthin II, Cathasterone, Oleanolic acid, Colnelenic acid, and Soraphen A were significantly upregulated, while metabolites like N-Fluorenylacetamide, Dihomomethionine, Bentazon, 15-keto lloprost, and Ammeline were significantly downregulated (Figure 4F). Among these differential metabolites, the three pennycress lines shared compounds enriched with Portulacaxanthin II (a carotenoid with anti-inflammatory and antioxidant activities), Oleanolic acid (an important plant secondary metabolite), and Soraphen A (a polyketide macrolide antibiotic produced by Myxobacteria).

To elucidate specific metabolic changes in the pennycress rhizosphere, pathway enrichment analysis was performed using the KEGG database on the differential metabolite sets from each of the three lines. The biosynthesis of type II polyketide products emerged as the most significantly altered pathway across all three pennycress lines (Figure 5G-I). Additionally, the pathways “Neomycin, kanamycin, and gentamicin biosynthesis” and “Biosynthesis of 12-, 14-, and membered macrolides” were consistently and significantly enriched in HeL43 among all groups (Supplementary Figures 7 and 8).

 doi:10.20944/preprints202602.0643.v1



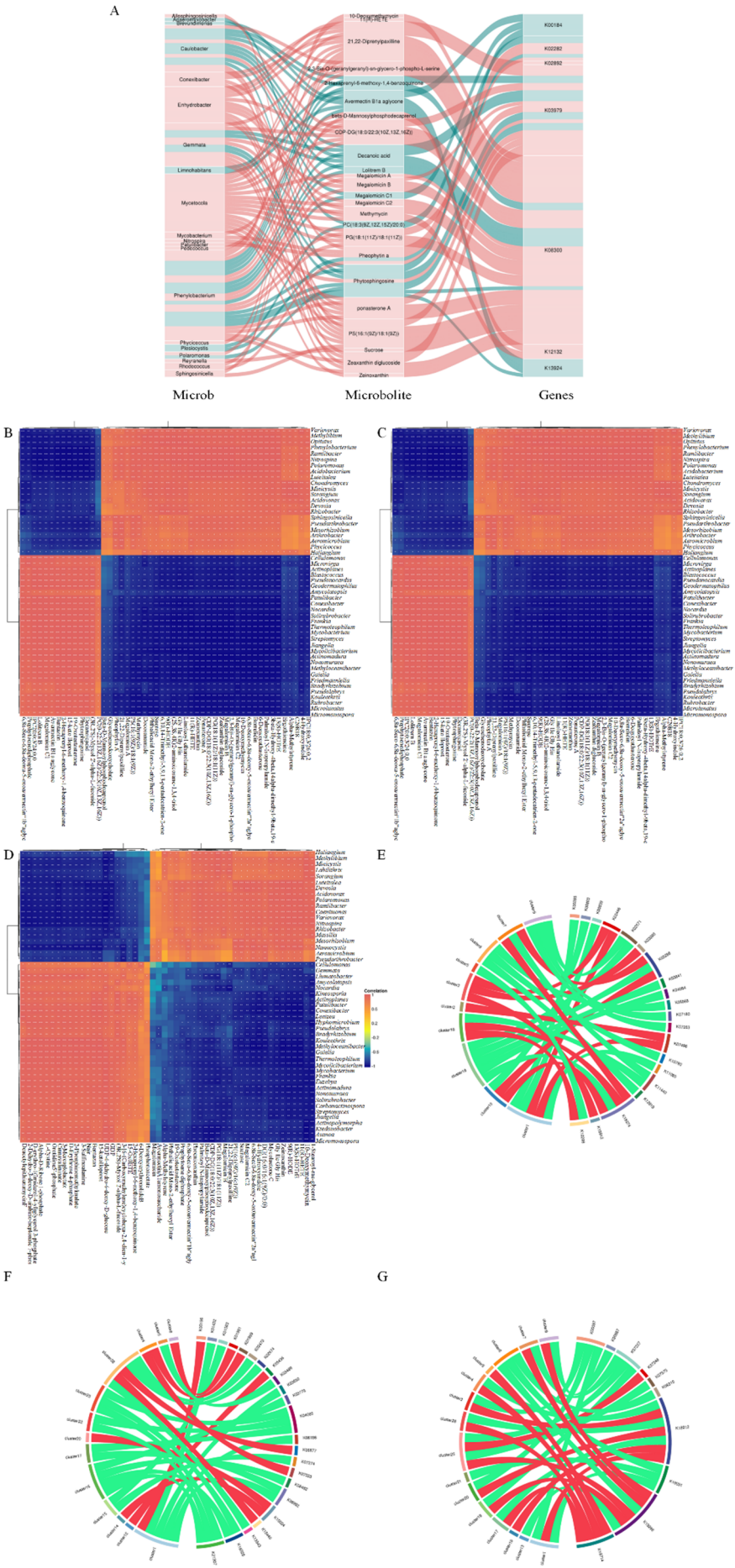

 doi:10.20944/preprints202602.0643.v1



**Figure 5.** Integrated analysis of soil microorganisms and metabolites. (A) Sankey diagram of species-functional gene-metabolite associations. The left column lists microbial species, the middle column lists metabolites, and the right column lists functional genes. Connections between species and metabolites, and between functional genes and metabolites, indicate significant correlations (red denotes positive correlation, green denotes negative correlation). (B) Heatmap correlating the abundance of differentially abundant metabolites and microorganisms in JiL67. (C) Heatmap correlating the abundance of differentially abundant metabolites and microorganisms in LiN54. (D) Heatmap correlating the abundance of differentially abundant metabolites and microorganisms in HeL43. Rows represent differentially abundant microbial species; columns represent differentially abundant metabolites. (E) String diagram of metabolite-microbial species-functional gene correlations for JiL67. (F) String diagram of metabolite-microbial species-functional gene correlations for LiN54. (G) String diagram of metabolite-microbial species-functional gene correlations for HeL43. The left half of the string diagram represents metabolites, while the right half represents microbial species. A wider string width indicates a higher frequency of association with that metabolite or microorganism.

### *3.6. Joint Analysis of Soil Microorganisms and Metabolites*

To explore the associations among differential metabolites, microorganisms, and functional genes, a Sankey diagram was constructed for microbial species–functional gene–metabolite correlation analysis ($|r| > 0.8$, $p < 0.05$; Figure 5A). Overall, the correlation networks exhibited more positive than negative links. The microbial species Phenylobacterium, Caulobacter, Mycetocola, and Gemmate displayed the highest number of significant correlations with differential metabolites, while metabolite 21,22-Diprenylpaxilline and PS (16:1(9Z)/18:1(9Z)) were most closely linked to a variety of microbial species. Notably, nearly all significant differential metabolites were associated with the functional gene K08300 (ribonuclease E [EC:3.1.26.12]) in the RNA degradation pathway.

Pearson correlation analysis was performed to assess the relationship between the abundances of differential metabolites and microbial taxa, with corresponding heatmaps generated. Among the 50 bacterial genera most strongly correlated with differential metabolites, each genus in JiL67 was significantly correlated with metabolites such as Sucrose, 11(R)-HETE, 15-keto lloprost, Bentazon, and 13(S)-HOTrE (Figure 5B). In LiN54, genera were most significantly correlated with metabolites 11(R)-HETE, 15-keto lloprost, Bentazon, 15-Oxo-ETE, and Glycochenodeoxycholate (Figure 5C), while in HeL43, the genera showed significant correlation with metabolites 9(R)-HODE, 11(R)-HETE, 15-keto lloprost, Bentazon, and 13(S)-HOTrE (Figure 5D). The metabolites 11(R)-HETE, 15-keto lloprost, and Bentazon appeared to be closely associated with microbial communities during pennycress cultivation.

A joint analysis of metabolites and functional genes was conducted using hierarchical clustering and correlation analysis. A chord diagram was constructed to visualize the associations between the top 30 differential metabolites and functional genes. In JiL67, the greatest number of metabolites showed significant correlations with K18074 (terephthalate 1,2-dioxygenase oxygenase component alpha subunit [EC:1.14.12.15]), and most of these correlations were positive (Figure 5E). In LiN54, most metabolites were significantly correlated with K04065 (hyperosmotically inducible periplasmic protein) and K21307 (sulfite dehydrogenase (quinone) subunit SoeA [EC:1.8.5.6])—both from the phylum Actinobacteria—and these correlations were predominantly negative (Figure 5F). In HeL43, the largest number of metabolites correlated significantly with K18912 (gamma-glutamyl hercynylcysteine S-oxide synthase [EC:1.14.99.50]), with a predominance of positive correlations (Figure 5G).

## 4. Discussion

### *4.1. Effects of Pennycress Lines on the Rhizosphere Microbial Community Structure*

The rhizosphere, influenced by root exudates, exhibits significant differences in microbial community abundance and diversity compared to the bulk soil matrix [27]. Among these, plant allelopathic effects significantly alter the structure and biological activity of rhizosphere microbial

 doi:10.20944/preprints202602.0643.v1



communities [28,29]. Pennycress, known for its strong allelopathic effects [30], significantly altered the soil microbial communities upon cultivation. Compared to the bulk soil control (CK), all three pennycress lines exhibited notable differences in their associated microbial communities. The alpha diversity of the rhizosphere community in JiL67 remained stable, whereas it decreased in LiN54. Conversely, HeL43 exhibited increased diversity along with signs of community homogenization. These findings suggest that the pennycress line is the primary factor driving the distinct rhizosphere microbiome structures observed among the groups [31,32].

The rhizosphere microbial community in this study was dominated by Proteobacteria, Actinobacteria, and Acidobacteria, which aligns with previous research [33,34]. Following pennycress cultivation, the relative abundances of Acidobacteria and Nitrospirae, along with the dominant Proteobacteria, were significantly higher than those in the bulk soil control (CK). These phyla are recognized for their adaptability and role in decomposing complex organic matter, contributing significantly to soil carbon balance [35–37]. Their enrichment suggests enhanced environmental adaptability in pennycress-treated soil.

Predictive analysis of metagenomic data revealed that, after pennycress cultivation, the rhizosphere microbial community exhibited significantly higher relative abundances of genes related to ketone body synthesis and degradation, aminobenzoate degradation, fluorobenzoate degradation, and polycyclic aromatic hydrocarbon degradation. This indicates an enhanced capacity for fat metabolism and the breakdown of aromatic compounds. The enrichment of pathways such as propanoate metabolism, valine, leucine, and isoleucine degradation, and fatty acid metabolism in LiN54 suggests that its rhizosphere is involved in energy metabolism and the decomposition and utilization of complex organic carbon sources. Additionally, the enrichment of 2-oxocarboxylic acid metabolism, RNA degradation, and pyrimidine metabolism in LiN54 indicates that its rhizosphere is engaged in central metabolism and genetic material turnover, essential for maintaining fundamental cellular processes and dynamic equilibrium.

In HeL43, the order Micrococcales was a primary contributor, known for its roles in nitrogen cycling [38], organic matter degradation, glucose utilization [39], and bioremediation [40]. Furthermore, the rhizosphere of HeL43 also harbored a higher abundance of bacteria associated with alkaloid degradation, such as *Arthrobacter*, *Variovorax*, and *Nocardioides* [36,41], along with the predicted enrichment of pathways related to microbial metabolism in diverse environments, pyruvate metabolism, and glyoxylate and dicarboxylate metabolism. This combined microbial profile may be attributed to the higher alkaloid content in HeL43 compared to the other lines. Moreover, in the pennycress rhizosphere, Nitrospirae was positively correlated with putative beneficial taxa such as Acidobacteria and Candidatus Rokubacteria. This correlation suggests that the microbial community may have gained functional efficiency and stability following pennycress cultivation.

### *4.2. Effects of Pennycress Lines on the Rhizosphere Soil Metabolome*

Metabolite analysis revealed differences in rhizosphere metabolites among the pennycress lines. PCA indicated that pennycress cultivation significantly altered the soil metabolic composition, further distinguishing the metabolic profiles of the different lines. Compared to CK, the rhizospheres of the three pennycress-planted groups were enriched in specific metabolites: Portulacaxanthin II (a terpenoid known for enhancing plant stress resistance and antioxidant capacity [42,43]), Oleanolic acid (a pentacyclic triterpenoid with anti-inflammatory and antibacterial properties [44,45]), and Soraphen A (a polyketide macrolide antibiotic produced by myxobacteria, exhibiting potent antibacterial activity [46]). Among these, 24-methylidenecycloartanol (a terpenoid linked to plant stress resistance [47]), which was abundant in the JiL67 line, and the significantly downregulated nebramycin factor 4 (an aminoglycoside antibiotic [48]), collectively suggest a shift in the rhizosphere from intense microbial antagonism to an adaptive mode dominated by plant structural reinforcement. In the LiN54 line, the rhizosphere was enriched with cytosine (a nitrogenous heterocyclic compound derived from nucleic acid degradation [49]), while the exogenous pollutant Ammeline [50] was significantly downregulated. This pattern indicates that the soil is transitioning

 doi:10.20944/preprints202602.0643.v1



from a disturbed to a more bioactive and healthy state. In the HeL43 line, the increased abundance of cytosine, coupled with the downregulation of Dihomomethionine (a sulfur-containing amino acid), suggests active metabolic and stress-resistant processes [51].

### *4.3. Correlation Between the Soil Metabolome and the Microbial Community*

Association analysis between microbial taxa, functional genes, and metabolites revealed strong links between differential soil metabolites and microbial communities. The concurrent enrichment of Phenylobacterium (an efficient degrader of aromatic compounds [52]) and the fungal metabolite 21,22-diprenylpaxilline (an indole diterpenoid alkaloid) points to active fungal-bacterial chemical interplay in the pennycress rhizosphere. KEGG enrichment analysis of these metabolites identified the biosynthesis of type II polyketide products (a fungal-associated pathway for broad-spectrum antibiotics [53,54]) as the most significantly altered. Together with the co-enrichment of *Mycetocola* (known for its close fungal associations), this suggests a substantial enhancement of the soil microbiome's potential antibacterial function following pennycress cultivation.

Additionally, *Caulobacter* (specializing in attachment under oligotrophic conditions [55]) and *Gemmate* (a fast-growing bacterium potentially symbiotic with *Nocardioides* [56]) were significantly associated with the high abundance of PS (16:1(9Z)/18:1(9Z)), a marker lipid for apoptosis, and ribonuclease E in the rhizosphere soil [57]. This suggests that the pennycress rhizosphere may establish an efficient organic nutrient recycling system driven by specific microbes, underpinned by high rates of cellular turnover. Both 21,22-diprenylpaxilline and PS (16:1(9Z)/18:1(9Z)) were positively correlated with all differentially abundant microbial taxa. Since many of these genera promote plant growth, this indicates that higher levels of these metabolites could enhance the proliferation of beneficial genera in the rhizosphere soil. In HeL43, which exhibited higher total alkaloid content, the concentrations of Portulacaxanthin II and Oleanolic acid in the rhizosphere soil were significantly elevated. This suggests that increased alkaloid synthesis in this group may alter the composition of root exudates, exerting selective pressure on the rhizosphere microbial community and specifically enriching microorganisms with alkaloid tolerance/degradation abilities and specific secondary metabolic potential (e.g., *Arthrobacter*, *Variovorax*, *Nocardioides*). Concurrently, the upregulation of genes related to the synthesis and degradation of ketone bodies and the biosynthesis of type II polyketide products suggests that microbes redirected carbon flux, leading to the enrichment of Soraphen A—an antibiotic polyketide macrolide with both antibacterial and herbicidal properties—in the rhizosphere.

While this study has hypothesized connections between some metabolites and microorganisms, the interactions among microbes remain inadequately explored. Future research could be strengthened by integrating enzymatic activity assays in the pennycress rhizosphere and adopting a tripartite analytical framework linking microbes, enzymes, and metabolites. This approach would provide more comprehensive insights into enhancing soil quality and optimizing pennycress agronomic practices.

## 5. Conclusion

This study integrated metagenomics and rhizosphere metabolomics to characterize the microbiome and metabolome of pennycress rhizosphere soil. HeL43, which exhibits a higher total alkaloid content, likely exerts strong selection pressure in its rhizosphere, thereby enriching specific microbial taxa with alkaloid tolerance. These enriched microbes may adapt to this chemical stress by reshaping their metabolomes and activating specific secondary metabolic pathways, such as antibiotic biosynthesis pathways, thus gaining a competitive advantage in the rhizosphere. In summary, inter-varietal differences in secondary metabolites, particularly alkaloids, represent a key driver of the lineage-specific assembly of the pennycress rhizosphere microbiome. Our findings provide novel insights into the metabolite-mediated interactions between pennycress lines and their associated rhizosphere communities.

 doi:10.20944/preprints202602.0643.v1



**Supplementary Materials:** Table S1: Field pennycress rhizosphere soil microbial metagenome sequencing data statistics; Table S2. Difference significance analysis results of metabolite; Figure S1: Dilution curve of sample microbial communities; Figure S2: Species inter-sample distance boxplot. The vertical axis represents the Beta distance. The box plot above "Between" indicates the Beta distance data for all inter-group samples, while the subsequent box plots show the Beta distance data for intra-group samples within different groupings. In the Anosim analysis, an R-value closer to 1 suggests that inter-group differences are greater than intra-group differences, whereas a smaller R-value indicates no significant distinction between inter-group and intra-group differences. A P-value less than 0.05 indicates high reliability of the test; Figure S3: Inter-sample Correlation Heatmap; Figure S4: Volcano plot of differentially expressed metabolites for CK versus JiL67; Figure S5: Volcano plot of differentially expressed metabolites for CK versus LiN54; Figure S6: Volcano plot of differentially expressed metabolites for CK versus HeL43; Figure S7: Metabolic pathway enrichment analysis for JiL67 versus HeL43; Figure S8: Metabolic pathway enrichment analysis for LiN54 versus HeL43.

**Author Contributions:** Conceptualization, L. T.; methodology, W. Z.; software, L. Y.; validation, L. T. and Y. S.; formal analysis, W. Z; investigation, L. Y.; resources, L. T.; data curation, W. Z; writing—original draft preparation, W. Z. and C. F.; writing—review and editing, L. T. and Y. S.; visualization, W. Z.; supervision, C. F.; project administration, C. F.; funding acquisition, L. T. All authors have read and agreed to the published version of the manuscript.

**Funding:** The China Agriculture Research System of MOF and MARA (CARS-16-S3).

**Data Availability Statement:** Raw readings of metagenomic and metabolomic data were submitted to the Sequence Read Archive (SRA) for the NCBI database (Accession Number: PRJCA041574 and PRJCA051630).

**Conflicts of Interest:** The authors declare no conflicts of interest.

## References

1. McGinn, M.; Phippen, W.B.; Chopra, R.; Bansal, S.; Jarvis, B.A.; Phippen, M.E.; Dorn, K.M.; Esfahanian, M.; Nazarenus, T.J.; Cahoon, E.B., Durrett, T.P., Marks, M.D., Sedbrook, J.C. Molecular tools enabling pennycress (*Thlaspi arvense* L.) as a model plant and oilseed cash cover crop. *Plant Biotechnology Journal*. 2019, 17(4), 776-788.
2. Langdale, G.W.; Blevins, R.L.; Karlen, D.L.; McCool, D.K.; Nearing, M.A.; Skidmore, E.L. Cover crop effects on soil erosion by wind and water. In: *Cover crops for clean water* (Ankeny, Iowa: Soil and Water Conservation Society). 1991, pp. 15–21.
3. Gyssels, G.; Poesen, J.; Bochet, E.; Li, Y. Impact of plant roots on the resistance of soils to erosion by water: a review. *Progress in Physical Geography*. 2005, 29(2), 189–217.
4. Dunn, M.; Ulrich-S, J.D.; Prokopy, L.S.; Myers, R.L.; Watts, C.R.; Scanlon, K. Perceptions and use of cover crops among early adopters: findings from a national survey. *Journal of Soil & Water Conserv*. 2016, 71(1), 29–40.
5. Han, E.; Li, F.; Perkons, U.; Küpper, P.M.; Bauke, S.L.; Athmann, M.; Thorup-Kristensen, K.; Kautz, T.; Köpke, U. Can precrops uplift subsoil nutrients to topsoil? *Plant and Soil*. 2021, 463, 329–345.
6. Marcus, G.; E, A.L.; L, S.G.; M, N.M.; Y, E.M.; N, C.T. A temporal analysis and response to nitrate availability of 3D root system architecture in diverse pennycress (*Thlaspi arvense* L.) accessions. *Frontiers in plant science*. 2023, 14, 1145389-1145389.
7. Winthrop-B, P.; Phippen, M.-E. Soybean seed yield and quality as a response to field pennycress residue. *Crop Science*. 2012, 52(6), 2767-2773.
8. Terry-A, I. US effort in the development of new crops (Lesquerella, PennycressCoriander and Cuphea). *Oléagineux, Corps, Lipides*. 2009, 16(4-5-6), 205-210.
9. Zanetti, T.; Isbell, T.A. ; Gesch, R.W. ; Evangelista, R.L; Alexopoulou, E.; Moser, B.; Monti, A. Turning a burden into an opportunity: Pennycress（*Thlaspi arvense* L.）a new oilseed crop for biofuel production. *Biomass and Bioenergy*. 2019, 130, 105354.
10. Li, X.J. Study on anti-inflammayory activity of *Thlaspi arvense* L. extract and 8 flavonoids. Nanning: Guangxi University, 2020.

 doi:10.20944/preprints202602.0643.v1




11. Xue, Y.; Zhang, L.C; Hu, W.; Jia, T.T.; Zhu, J.M.; Zhu, W.K.; Zhu, H.H. Herbal textual research of *Thlaspi* Herba. *Shanghai Journal of Traditional Chinese Medicine*. 2023, 57(10), 48-53.
12. Tnde, P.; Holb, I.J.; I, S.N.P. Secondary metabolites in fungus-plant interactions. *Frontiers in Plant Science*. 2015, 6573.
13. Li, C.Y.; Zha, W.J.; Li, W.; Wang, J.Y.; You, A.Q. Advances in The Biosynthesis of Terpenoids and Their Ecological Functions in Plant Resistance. *International Journal of Molecular Sciences*. 2023, 24(14), 11561-11561.
14. Ali, J.; Tonğa, A.; Islam, T.; Mir, S.; Mukarram, M.; Konôpková, A.S.; Chen, R. Defense Strategies and Associated Phytohormonal Regulationin Brassica Plants in Response to Chewing and Sap-Sucking Insects. *Frontiers in Plant Science*. 2024, 15, 1376917-1376917.
15. Wei, Y.F.; Qin, R.L.; Ding, D.C.; Li, Y.B.; Xie, Y.Y.; Qu, D.C.; Zhao, T.Y.; Yang, S.D. Structural characteristics of soil microbial community in rhizospheres of tomatoes during different growth periods. *Journal of Huazhong Agricultural University*. 2024, 43(1), 9-21.
16. Li, X.N.; Dai, W.Z.; Lin, X.R.; Liao, L.Y.; Lu, W.; Yang, S.D. Differential analysis in the structure of rhizosphere microbialcommunities and identification of functional taxa associated with the content of capsaicin in pepper varieties. *Journal of Huazhong Agricultural University*. 2016, 1-12.
17. Raza, W.; Jiang, G.F.; Eisenhauer, N., Huang, Y.H.; Wei, Z.; Shen, Q.R.; Kowalchuk, A.G.; Jousset, A. Microbe-induced phenotypic variation leads to over yielding in clonal plant populations. *Nature Ecology & Evolution*. 2024, 8(3), 392-399.
18. Zhou, X.G.; Zhang, J.Y.; Khashi., U.R.M.; Gao, D.M.; Wei Z.; Wu F.Z.; DiniAndreote, F. Interspecific plant interaction via root exudates structures the disease suppressiveness of rhizosphere microbiomes. *Molecular plant*. 2023,16(5), 849-864.
19. Wang, B.; Chen, C.; Xiao, Y.M.; Chen, K.Y.; Wang, J.; Zhao, S.; Liu, N.; Li, J.N.; Zhou, G.Y. Trophic relationships between protists and bacteria and fungi drive the biogeography of rhizosphere soil microbial community and impact plant physiological and ecological functions. *Microbiological Research*. 2024, 280, 127603.
20. Liu, J.W.; Li, X.Z.; Yao, M.J. Research progress on assembly of plant rhizosphere microbial community. *Acta microbiologica Sinica*. 2021, 61(2), 231-248.
21. Xu, J.; Zhang, Y.Z.; Zhang, P.F.; Trivedi, P.; Riera, N.; Wang, Y.Y.; Liu, X.; Fan, G.Y.; et al. The structure and function of the global citrus rhizosphere microbiome. *Nature communications*. 2018, 9(1), 4894.
22. Gao, C.; Montoya, L.; Xu, L.; Madera, M.; Hollingsworth, J.; Purdom, E.; Singan, V.; Vogel, J.; Hutmacher, R.B.; Dahlberg, J.A.; Coleman-Derr, D.; Lemaux, P.G.; Taylor, J.W. Fungal community assembly in drought-stressed sorghum shows stochasticity, selection, and universal ecological dynamics. *Nature communications*. 2020, 11(1), 34.
23. Zhou, Y.; Yi, S.X.; Zang, Y.; Yao, Q.; Zhu, H.H. The predatory myxobacterium *Citreicoccus inhibens* gen. nov. sp. nov. showed Antifungal Activity and Bacteriolytic Property against Phytopathogens. *Microorganisms*. 2021, 9(10), 2137.
24. Li, L.; Rodriguez-Concepcion, M.; Al-Babili, S. Recent advances in understanding carotenoid-derived signaling molecules in regulating plant growth and development. *Frontiers in Plant Science*. 2015, 6790.
25. Pang, Z.Q.; Chen, J.; Wang, T.H.; Gao, C.S.; Li, Z.M.; Guo, L.T.; Xu, J.P.; Cheng, Y. Linking plant secondary metabolites and plant microbiomes: a review. *Frontiers in Plant Science*. 2021, 12, 621276.
26. Liu, C.C.; Yu, J.S.; Ying, J.Z.; Zhang, K.; Hu, Z.G.; Liu, Z.X.; Chen, S.L. Integrated metagenomics and metabolomics analysis reveals changes in the microbiome and metabolites in the rhizosphere soil of Fritillaria unibracteata. *Frontiers in Plant Science*. 2023, 14, 1223720.
27. Zhang, L.; Xu, H.M.; Zhu, B.L. Association of rhizosphere soil microbiome with the occurrence and development of replant disease - A review. *Acta Microbiologica Sinica*. 2016, 56(8), 1234-1241.
28. Zhao, Y.X.; Zhou, J.Y.; Chen, L.L.; Li, S.; Yin, Y.; Jeyaraj, A.; Liu, S.J.; Zhuang, J.; Wang, Y.H.; Chen, X.; Li, X.H. Allelopathic Effect of Osmanthus fragrans Changes the Soil Microbial Community and Increases the Soil Nutrients and the Aroma Quality of Tea Leaves. *Journal of agricultural and food chemistry*. 2025, 73(22), 13818-13831.
29. Xu, Y.; Tan, Z.R.; Yin, Y.; Hua, J.M.; Han, Y.X.; Lin, J.X.; Wang, A.; Wang, J.H. Research progress on the effects of invasive plants on soil characteristics. *Chinese Journal of Plant Ecology*. 2025,49(11), 1767-1777.

 doi:10.20944/preprints202602.0643.v1




30. Zhang, H.; Ma, R.J.; Wang, N.L.; Li, G. Allelopathic Effects of Different Plants on the Major Weed *Ligularia sagitata* in Alpine and Cold Grassland. *Acta Botanica Boreali-Occidentalia Sinica*. 2006, (11), 2307-2311.
31. Bressan, M.; Roncato, M-A.; Bellvert, F.; Comte, G.; Haichar, F.E.; Achouak, W.; Berge, O. Exogenous glucosinolate produced by *Arabidopsis thaliana* has an impact on microbes in the rhizosphere and plant roots. *The ISME Journal*. 2009, 3(11), 1243–1257.
32. Aleklett, K.; Leff, J.; Fierer, N.; Hart, M. Wild plant species growing closely connected in a subalpine meadow host distinct root-associated bacterial communities. *PeerJ*. 2015, 3(8), e804.
33. Zeng, W.A.; Yang, Z.Y.; Huang, Y.; Gu, Y.B.; Tao, J.M.; Liu, Y.J.; Xie, P.F.; Cai, H.L.; Yin, H.Q. Response of soil bacterial community structure and co-occurrence network topology properties to soil physicochemical properties in long-term continuous cropping farmland. *Acta Microbiological Sinica*. 2022, 62(06), 2403-2416.
34. Pham, H.N.; Pham, P.A.; Nguyen, T.T.H.; Meiffren, G.; Brothier, E.; Lamy, I.; Michalet, S.; Dijoux-Franca, M.G.; Nazaret, S. Influence of metal contamination in soil on metabolic profiles of Miscanthus × giganteus belowground parts and associated bacterial communities. *Applied Soil Ecology*. 2018, 125, 240-249.
35. Xiao, D.; Huang, Y.; Feng, S.Z.; Ge, Y.H.; Zhang, W.; He, X.Y.; Wang, K.L. Soil organic carbon mineralization with fresh organic substrate and inorganic carbon additions in a red soil is controlled by fungal diversity along a pH gradient. *Geoderma*. 2018, 321, 79-89.
36. Chen, L.F.; He, Z.B.; Zhao, W.Z.; Kong, J.Q.; Gao, Y. Empirical evidence for microbial regulation of soil respiration in alpine forests. *Ecological Indicators*. 2021, 126, 107710.
37. Zhang, Z.X.; Li, J.H.; Zhang, L.N.; Su, M.; Chen, J.; Yang, Z.P.; Gao, Z.Q.; Qiao, Y.J.; Zhang, X.Y.; Xue, Z.Q.; Zhang, C.L. Effects of combined application of selenium and nitrogen fertilizers on selenium and nitrogen accumulation in oat plants, rhizospheric soil microbial community, and metabolites. *Chinese Journal of Applied and Environmental Biology*. 2023, 29(05), 1241-1252.
38. Yang, J.; Lin, Y.; Yang, W.H.; Zhou, B.Q.; Mao, Y.L.; Xing, S.H. Soluble organic nitrogen variation rate and its response to bacteria under different fertilization treatments in paddy soil. *Journal of Agro-Environment Science*. 2021, 40(07), 1509-1518.
39. Montel, M.C.; Reitz, J.; Talon, R.; Berdague, J.; Rousset-Akrim, S. Biochemical activities of Micrococcaceae and theireffects on the aromatic profiles and odours of a dry sausage model. *Food Microbiology*. 1996, 13(6), 489-499.
40. Fan, Q.S.; Wanapat, M.; Hou, F.J. Chemical composition of milk and rumen microbiome diversity of yak, Impacting by herbage grown at Different Phenological Periods on the Qinghai-Tibet Plateau. *Animals*. 2020, 10(6), 1030.
41. Vandera, E.; Samiotaki, M.; Parapouli, M.; Panayotou, G.; Koukkou, A.I. Comparative proteomic analysis of Arthrobacter phenanthrenivorans Sphe3 on phenanthrene, phthalate and glucose. *Journal of Proteomics*. 2015, 113, 73-89.
42. Yin, L.; Liu, J.X.; Tao, J.P.; Xing, G.M.; Tan, G.F.; Li, S.; Duan, A.Q.; Ding, X.; Xu, Z.S.; Xiong, A.S. The gene encoding lycopene epsilon cyclase of celery enhanced lutein and β-carotene contents and confers increased salt tolerance in Arabidopsis. *Plant Physiology and Biochemistry*. 2020, 157, 339-347.
43. Tian, L. Recent advances in understanding carotenoid-derived signaling molecules in regulating plant growth and development. *Frontiers in Plant Science*. 2015, 6, 790.
44. Priyanka, M.; Asit, R.; Sudipta, J.; Sanghamitra, N.; Sujata, M. Influence of extraction methods and solvent system on the chemical composition and antioxidant activity of *Centella asiatica* L. leaves. *Biocatalysis and Agricultural Biotechnology*. 2021, 33, 101971.
45. Renju, K; John, J.A.; Sabulal, B. Centella asiatica: secondary metabolites, biological activities and biomass sources. *Phytomedicine Plus*. 2022, 2(1), 100176.
46. Dipesh, D.; Thi, L.; Prasad, R.; Kumar, J.; RitBahadur, G.; Prakash, P.; Raj, P.A.; Cheol, Y.J.; Kyung, S.J. Enhanced production of nargenicin A (1) and generation of novel glycosylated derivatives. *Applied biochemistry and biotechnology*. 2015, 175(6), 2934-2949.
47. Thimmappa, R.; Geisler, K.; Louveau, T.; O'Maille, P.; Osbourn, A. Triterpene Biosynthesis in Plants. *Annual Review of Plant Biology*. 2014, 65(1), 225-257.

 doi:10.20944/preprints202602.0643.v1




48. Han, L.X; Zhang, H.P.; Long, Z.N.; Ge, Q.Q.; Mei, J.J.; Yu, Y.L.; Fang, H. Exploring microbial community structure and biological function in manured soil during ten repeated treatments with chlortetracycline and ciprofloxacin. *Chemosphere*. 2019, 228, 469-4777.
49. Zhang, F.S.; Wang, J.Q.; Zhang, W.F.; Cui, Z.L.; Ma, W.Q.; Chen, X.P.; Jiang, R.F. Nutrient Use Efficiencies of Major Cereal Crops in China and Measures for Improvement. *Acta Pedologica Sinica*. 2008, 05, 915-924.
50. Kazuhiro, T.; Kunihiko, F.; Ken-ichi, Y.; Naoki, H.; Akio, I. Biodegradation of melamine and its hydroxy derivatives by a bacterial consortium containing a novel *Nocardioides* species. *Applied microbiology and biotechnology*. 2012, 94(6), 1647-1656.
51. Khan, M.; Iqbal, N.; Masood, A.; Mobin, M.; Anjum, N.A.; Khan, N.A. Modulation and significance of nitrogen and sulfur metabolism in cadmium challenged plants. *Plant Growth Regulation*. 2016, 78(1), 1-11.
52. Ullah, K.I.; Neeli, H.; Xiao, M.; Huang, X.; Ullah, K.N.; Wan-Taek, I.; Iftikhar, A.; Zhi, X.Y.; Li, W.J. *Phenylobacterium terrae* sp. nov., isolated from a soil sample of Khyber-Pakhtun-Khwa, Pakistan. *Antonie van Leeuwenhoek*. 2018, 111(10), 1767-1775.
53. Hoa, N.X.; Wai, N.K.; Seong, L.Y.; Hwan, K.Y.; Hak, M.J.; Yong, K.K. Antagonism of antifungal metabolites from Streptomyces griseus H7602 against Phytophthora capsici. *Journal of basic microbiology*. 2015, 55(1), 45-53.
54. Xiong, Z.Q.; Zhang, Z.P.; Li, J.H.; Wei, S.J.; Tu, G.Q. Characterization of Streptomyces padanus JAU4234, a producer of actinomycin X2, fungichromin, and a new polyene macrolide antibiotic. *Applied and Environ Microbiology*. 2012, 78(2), 589-592.
55. Tong, X.M, Chen, F, Yu, J, A, S.C.R.; L, S.J.B.; Wang, W.; Liang, Y.; Zheng, X.G.; Wang, J. Analysis of bacterial flora structure and diversity in snow on zhuoyou peak(8201m). *Chinese Science Bulletin*. 2008, 53(18), 2216-2222.
56. Qian, J.; Wu, Z.Y.; Zhu, Y.Z.; Zhang, Y.; Guo, X.K.; Liu, C. Correlation between microecology and antibiotic resistance atthe pig-soil interface in Chongming District, Shanghai, China. *Chinese Journal of Microecology*. 2024, 36(02), 135-146.
57. Akers, J.C.; Gonda, D.; Kim, R.; Carter, B.S.; Chen, C.C. Biogenesis of extracellular vesicles (EV): exosomes, microvesicles, retrovirus-like vesicles, and apoptotic bodies. *Journal of neuro-oncology*. 2013, 113(1), 1-11.